

# Electronic modulation of biochemical signal generation

Tanya Gordonov<sup>1,2</sup>, Eunkyong Kim<sup>2</sup>, Yi Cheng<sup>3,4</sup>, Hadar Ben-Yoav<sup>3,5</sup>, Reza Ghodssi<sup>3,5</sup>, Gary Rubloff<sup>3,4</sup>, Jun-Jie Yin<sup>6</sup>, Gregory F. Payne<sup>1,2</sup> and William E. Bentley<sup>1,2\*</sup>

**Microelectronic devices that contain biological components are typically used to interrogate biology<sup>1,2</sup> rather than control biological function. Patterned assemblies of proteins and cells have, however, been used for *in vitro* metabolic engineering<sup>3-7</sup>, where coordinated biochemical pathways allow cell metabolism to be characterized and potentially controlled<sup>8</sup> on a chip. Such devices form part of technologies that attempt to recreate animal and human physiological functions on a chip<sup>9</sup> and could be used to revolutionize drug development<sup>10</sup>. These ambitious goals will, however, require new biofabrication methodologies that help connect microelectronics and biological systems<sup>11,12</sup> and yield new approaches to device assembly and communication. Here, we report the electrically mediated assembly, interrogation and control of a multi-domain fusion protein that produces a bacterial signalling molecule. The biological system can be electrically tuned using a natural redox molecule, and its biochemical response is shown to provide the signalling cues to drive bacterial population behaviour. We show that the biochemical output of the system correlates with the electrical input charge, which suggests that electrical inputs could be used to control complex on-chip biological processes.**

The presented system uses electrical signals to assemble and tune an enzymatic pathway on a gold electrode chip, thereby creating a programmable hybrid device that contains both biological and electronic components. The electrical signals can control both the amount of assembled enzymes and their activity, the latter by oxidation through a diffusible redox mediator. The biohybrid device assembly process is electrically guided by electrodeposition (Fig. 1)<sup>13,14</sup>. The multidomain fusion protein HLPT<sup>7</sup> (Fig. 1b) was used as a model enzyme, and was covalently grafted onto a chitosan scaffold electrodeposited on a gold electrode chip (Fig. 1c). The chitosan film serves as a template for protein incorporation onto the device surface. HLPT consists of an N-terminal pentahistidine tag and the bacterial enzymes LuxS and Pfs, which are the two terminal synthases of bacterial autoinducer-2 (AI-2). This quorum-sensing (QS) signal molecule is normally secreted from cells to mediate a transition from individual cells to collective behaviour within bacterial populations, and promotes the establishment of biofilms<sup>14-16</sup>, among other phenotypes. Here, we look to use electric signals to mediate bacterial responses. HLPT also contains a C-terminal pentatyrine tag that allows covalent attachment to chitosan's primary amines via the enzyme tyrosinase<sup>17</sup>. These biofabrication assembly methods (Supplementary Section 3) have proven reliable in retaining enzymatic activity on chip and in providing an even protein coating (Fig. 3a)<sup>4,18</sup>.

After assembly, the desired biohybrid device will modulate the activity of HLPT for the guided synthesis of AI-2 and a by-product, homocysteine (Hcy) (1:1 stoichiometric ratio). On-chip enzyme activity was assayed using three modalities: optical, electrochemical and biological (Supplementary Section 4). The experiments were carried out at physiologically relevant concentrations; importantly, our methods are linear in these ranges, including a near real-time electrochemical method for Hcy. Applications that require real-time assessment and no sampling (direct *in situ* measurement) may thus be feasible (Supplementary Fig. 3).

HLPT oxidation can be mediated in several ways. Our initial studies made use of chemical oxidation via the powerful protein oxidant K<sub>2</sub>IrCl<sub>6</sub> (iridium, denoted Ir(IV))<sup>19</sup>. The results (Supplementary Figs 4 and 5; see discussion in Supplementary Section 6) indicate that oxidized iridium, and not its reduced form (controls), decrease HLPT activity in a predictable concentration- and time-dependent manner.

To test for electric actuation we selected the natural plant-based redox mediator acetosyringone (AS) ( $E_0 = +0.5$  V versus Ag/AgCl). AS is generated during the innate plant immune response to pathogens, and is then consumed in an oxidative burst<sup>20</sup>. It normally exists biologically in a reduced state (AS(R)). As can be seen in Fig. 2b, we observed the electric oxidation of AS through the simple evolution to a brownish-orange colour that is characteristic of the oxidized form<sup>21</sup>.

We next investigated whether electrically oxidized AS could oxidize HLPT (Fig. 2a), as well as the nature of that oxidation. LuxS has a divalent cation (Zn<sup>2+</sup>, Fe<sup>2+</sup>) at its active site, which could be a target for oxidation and attenuation of activity. Alternatively, sulfhydryl residues are more suitable targets for a generalized approach. AS(O) was added to HLPT, as well as to LuxS and Pfs, after which the oxidation status of the protein was measured. Our results indicate an approximately fourfold reduction in -SH groups (Fig. 2d; for details see Supplementary Section 7), showing that AS(O) has oxidized vulnerable sulfhydryl residues on all three proteins. These results were supported by the use of electron paramagnetic resonance (EPR) spectroscopy to demonstrate the protein's more general oxidation state. To detect general oxidation, we used the EPR probe CPH (1-hydroxy-3-carboxy-2,2,5,5-tetramethylpyrrolidine-HCl), which is oxidized by oxidized HLPT, so that its radical is revealed and detected. We measured a 2.5-fold increase in CPH radical from solutions where HLPT was treated with AS(O) (Fig. 2c). Additionally, using inductively coupled plasma optical emission spectroscopy (ICP-EOS), we found Zn<sup>2+</sup> was unaffected. In summary, our results demonstrate that HLPT

<sup>1</sup>Fischell Department of Bioengineering, University of Maryland, College Park, Maryland 20742, USA, <sup>2</sup>Institute for Bioscience & Biotechnology Research, University of Maryland, College Park, Maryland 20742, USA, <sup>3</sup>Institute for Systems Research, University of Maryland, College Park, Maryland 20742, USA, <sup>4</sup>Department of Materials Science and Engineering, University of Maryland, College Park, Maryland 20742, USA, <sup>5</sup>Department of Electrical and Computer Engineering, University of Maryland, College Park, Maryland 20742, USA, <sup>6</sup>Division of Analytical Chemistry, Office of Regulatory Science, Center for Food Safety and Applied Nutrition, US Food and Drug Administration, College Park, Maryland 20740, USA. \*e-mail: [bentley@umd.edu](mailto:bentley@umd.edu)

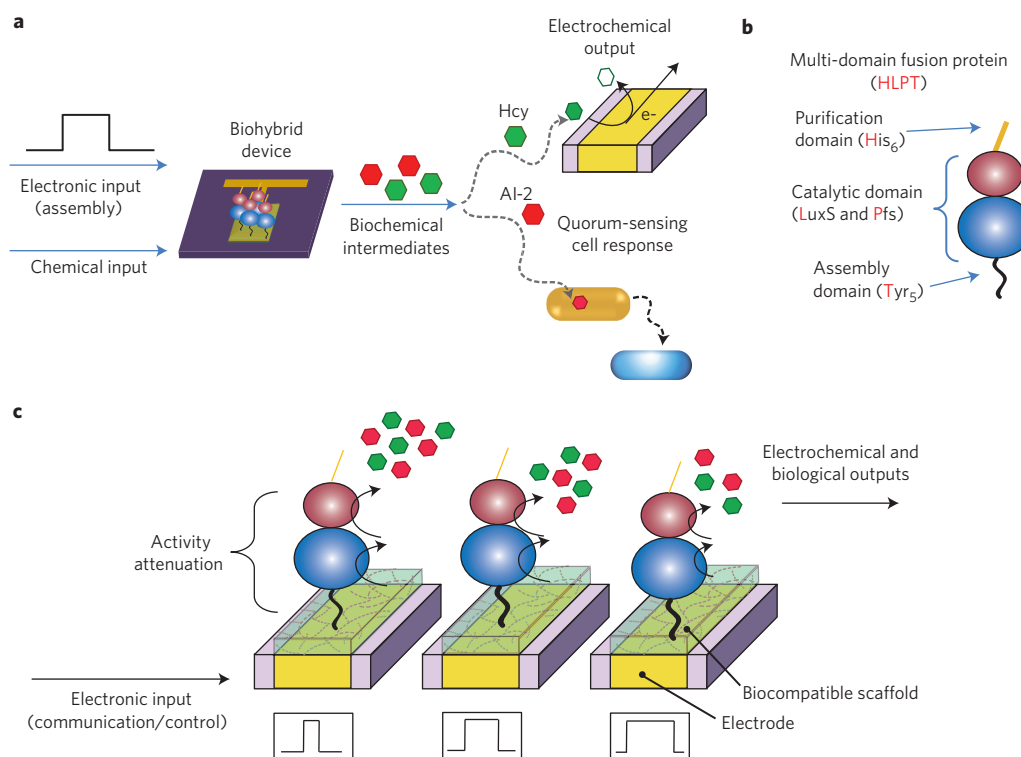


**Figure 1 | Schematic of the biohybrid device controlled by electronic signals. a**, Schematic of the biohybrid device receiving both chemical (enzyme reaction precursor) and electronic inputs, and, through biochemical intermediates, translating them to both electrochemical signals and biological cell responses. **b**, Representation of the components of the multidomain fusion protein (HLPT) used in the study. **c**, Experimental concept. By varying the electronic inputs through the electrodes on which the HLPT is attached, the attenuation of HLPT activity can be varied, thus affecting the electrochemical and biological responses in proportion to the input. Purple rectangles, silicon wafer; gold rectangles, patterned gold electrodes; semitransparent turquoise rectangles, biocompatible chitosan scaffold. Hcy, homocysteine; AI-2, autoinducer-2; His, histidine; Tyr, tyrosine. LuxS and Pfs are enzymes within HLPT.

activity is attenuated by the oxidation of its sulfhydryl residues and not by oxidation of the active-site cation. Our observations support the notion that on-chip activity could be controlled by exposure to AS(O), and that the methodology might be predictable.

To test whether the oxidation of HLPT by AS(O) affects activity, 1.5  $\mu\text{M}$  HLPT was treated with AS(O) as already described, then incubated with the enzyme pathway precursor *S*-adenosyl-homocysteine (SAH) (1 mM, 37 °C) (Supplementary Section 8). At the end of incubation (3–3.5 h), the amount of Hcy produced was measured and HLPT activity was calculated (Supplementary Section 5). Our results show that HLPT activity decreased linearly with exposure time and in proportion to the AS(O)/HLPT ratio (Fig. 2d, Supplementary Fig. 7), demonstrating that HLPT activity is attenuated by AS(O) oxidation, an electronically controlled process.

We next tested our main hypothesis—electrical assembly of HLPT on a chip and *in situ* activity attenuation. For these on-chip experiments, the biohybrid device (set-up assembled as described in Supplementary Sections 2, 3 and Methods) was immersed in a solution of AS(R), where it served as the working electrode. In a one-step process, the electrode was biased at +0.55 V, and the AS oxidized at the surface could react with the surface-bound HLPT (Fig. 3b, Supplementary Section 9). An amplified current output similar to that for solution-based oxidation was observed (Supplementary Fig. 8). To test our hypothesis that input charge correlates with decreased on-chip activity, both end-of-reaction and real-time measurements were performed. Enzyme-laden chips were biased at +0.55 V for different times (10–1,000 s, resulting in different levels of accumulated input charge and oxidation of AS), after which they were incubated with the SAH substrate as before

to allow Hcy and AI-2 generation. Enzyme activity was calculated, and a linear decrease was found followed by a plateau at long exposure times (Fig. 3c). Control reactions showed that both the oxidizing voltage (+0.55 V) and the presence of AS were needed for attenuation (Supplementary Fig. 8). The observed linear decrease supports the conclusion that as more AS is oxidized at the surface, it reacts with and oxidizes more HLPT on the electrode, reducing its activity proportionally. Correspondingly, this was dependent on the amount of active HLPT present, as can be seen from the three different series of chips, each with different initial activities. Also, Hcy increased nearly linearly with time, as indicated by our real-time measurement. Finally, these measurements correlated with our end-of-reaction samples (Supplementary Fig. 9).

We then estimated the apparent numbers of electrons needed to deactivate one HLPT molecule for each on-chip reaction (for calculations and discussion see Supplementary Section 10). We found this number (30–90) to be of the same order of magnitude as the predicted number of target sulfhydryl residues that could be oxidized on the protein complex (based on crystal structures<sup>22,23</sup>).

We then asked whether we could predictably tune the activity of an assembled enzyme complex to a specific ‘setpoint’. For these experiments (which are outlined and discussed in Supplementary Section 9) we used electronic signals to both load more than a sufficient amount of enzyme onto the chip and then tune the activity by calculating the needed charge and biasing the electrode for the estimated duration. In one envisioned application, this method might enable the design and real-time feedback control of flux through a surface-assembled biochemical pathway.

Finally, the principal motivation behind our concept was the ability of the biohybrid device to translate electrical signals to

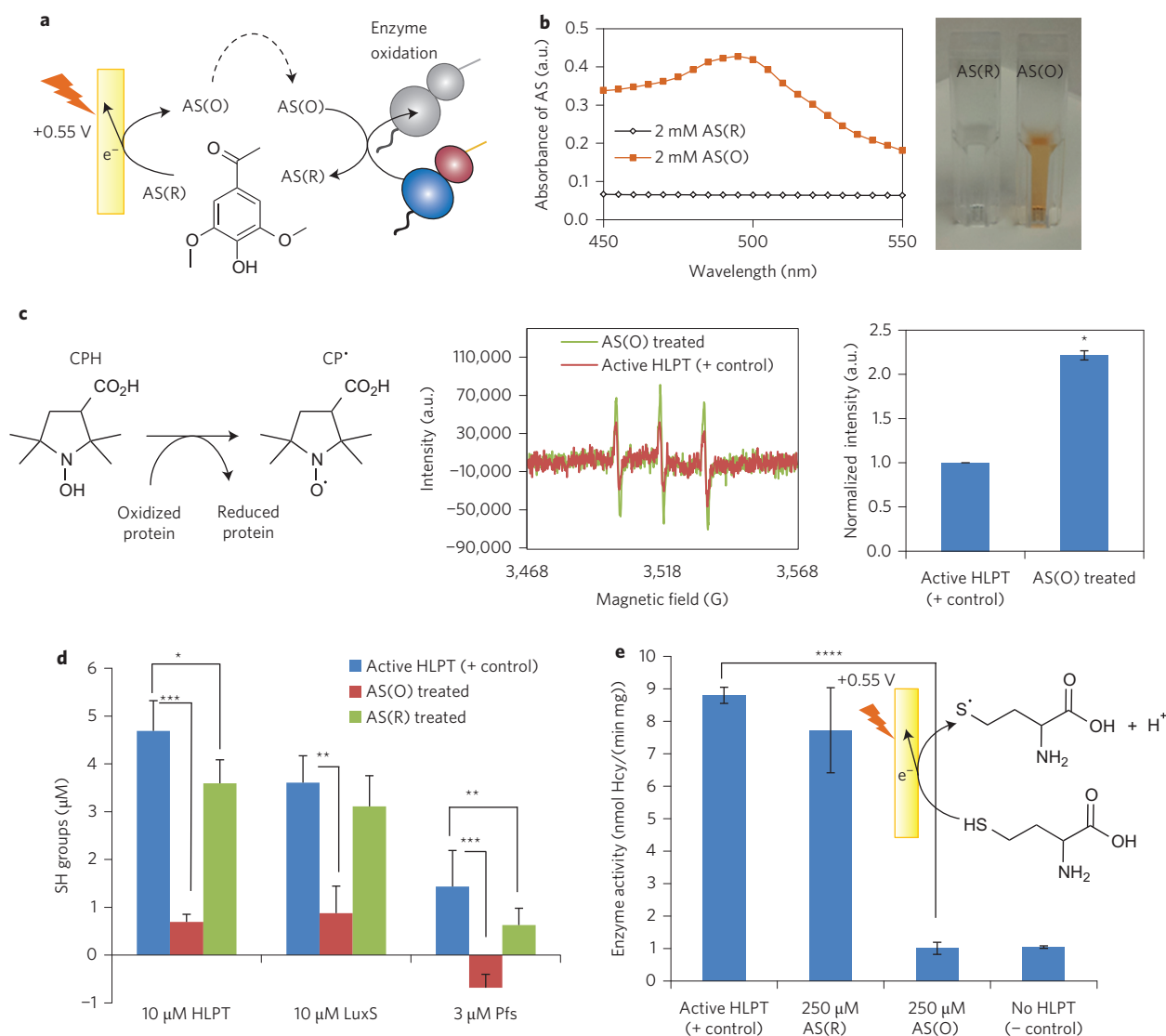


**Figure 2 | Electronically driven HLPT attenuation by natural mediator acetosyringone (AS).** **a**, Schematic of electrochemical oxidation of AS(R) in solution, followed by its addition to HLPT, where it oxidizes and attenuates HLPT activity and is reduced back to AS(R) in the process. **b**, Spectrophotometric measurements of AS(R) and AS(O). As AS is oxidized, it turns a brownish-orange colour, detectable at 490 nm. **c**, Oxidation of HLPT by AS(O) can be detected with the electron paramagnetic resonance (EPR) probe CPH, which is oxidized by the AS(O)-oxidized protein. A higher EPR intensity is seen when the protein is treated with AS(O). The EPR spectra show samples measured after 2 min of CPH reaction with protein. The bar graph represents an average of several normalized measurements (Supplementary Section 8). **d**, Sulfhydryl groups detected through Ellman's assay after treatment of the proteins with AS(O) or AS(R). **e**, HLPT activity calculated from electrochemical measurements after incubation with AS(O) or AS(R). Inset: Reaction of Hcy as it is oxidized at the electrode. Measurements in **c** were performed as described in Supplementary Section 8, in duplicate. Measurements in **d** and **e** were performed in triplicate. All error bars indicate s.d. Two-tailed, unequal variance student *t*-tests were run on data in **c**–**e**. \**P* < 0.05, \*\**P* < 0.01, \*\*\**P* < 0.001, \*\*\*\**P* < 0.0001. AS(R) and AS(O) are reduced or oxidized acetosyringone, respectively. CPH is the EPR spin probe 1-hydroxy-3-carboxy-2,2,5,5-tetramethylpyrrolidine-HCl. HLPT, fusion protein. LuxS and Pfs are the catalytic enzymes within HLPT.

modulate complex biological behaviour, including cell phenotype. We sought to demonstrate that on-chip modulation of HLPT affected the generation of both Hcy and AI-2, and then that AI-2 would affect the bacterial phenotype. In the present case this was demonstrated by the generation of a blue fluorescent protein among engineered *Escherichia coli* bacteria (Fig. 4a). We prepared HLPT-immobilized electrode chips as before, and applied varying amounts of charge to attenuate the enzymatic activity to different desired setpoints. As before, we allowed the enzymatic reaction to take place, and electrochemically measured the amount of Hcy generated. After exposing the cells to the solution containing AI-2, we used fluorescence-assisted cell sorting (FACS) to detect the blue fluorescent response (Supplementary Section 4).

Figure 4b presents FACS histogram plots of different fluorescence intensities resulting from HLPT-immobilized chips modulated using the indicated amounts of charge. Our results confirmed the electrically controlled generation of bacterial communication molecules (in the same proportion as Hcy) and similarly modulated biological signalling, as indicated by cell fluorescence (Fig. 4c). This meant that we could predict and feed forward control biological behaviour from our electrochemical Hcy measurements. Moreover, this first ever finding has shown that population-wide biological behaviour has been modulated electrically.

These combined results (Figs 3, 4 and Supplementary Figs 9, 10) suggest that AS(O)-driven on-chip electronic attenuation may be a predictable process for our biohybrid device, and support our

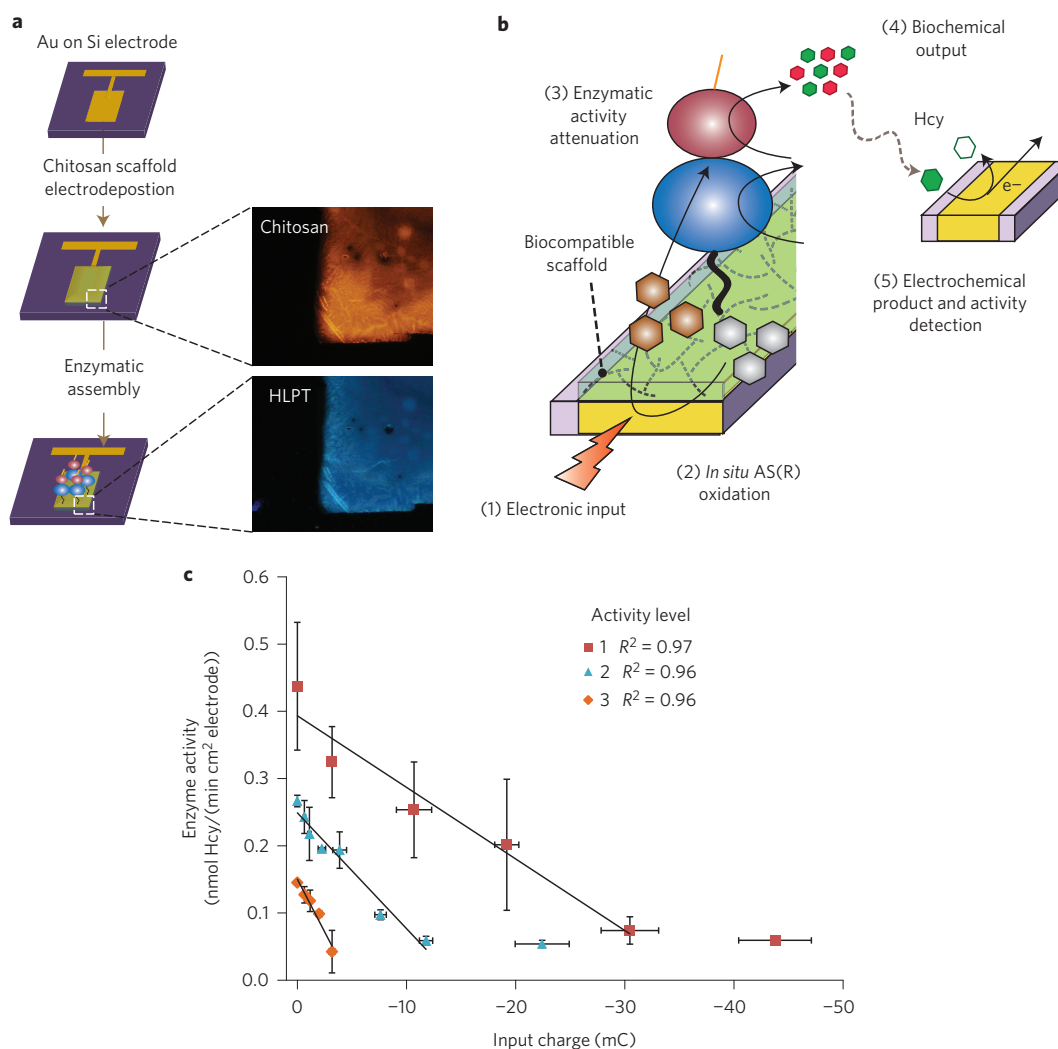


**Figure 3 | On-chip enzyme activity is linear with input charge.** **a**, Immobilization of enzyme onto a silicon chip involves chitosan electrodeposition as a thin film followed by enzymatic assembly of HLPT. Fluorescent pictures of red-labelled chitosan and blue-labelled HLPT show film and enzyme co-localization onto the gold-patterned electrode. **b**, Schematic depicting *in situ* enzyme attenuation. The same electrode on which the HLPT is attached is used to oxidize the AS (grey to brown hexagons) in the vicinity of the protein and leads to activity attenuation. Activity is then measured by electrochemical detection of Hcy (green hexagon) as described in the main text. **c**, Correlation between input charge applied for *in situ* AS oxidation as in **b** and the Hcy measured from HLPT thus attenuated at the end of 3.5 h incubation. Three series are depicted, with different initial enzymatic activities. There are two activity and four input charge measurements per data point. Error bars indicate s.d.  $R^2$  values indicate Pearson correlation coefficients for linearity for the displayed averaged data. Values for Pearson and Spearman rank coefficients for monotonic correlation for all non-averaged data are, respectively,  $-0.81$  and  $-0.91$  for activity level 1,  $0.92$  and  $-0.93$  for activity level 2, and  $0.92$  and  $-0.96$  for series 3. Hcy, homocysteine; mC, millicoulombs; HLPT, fusion protein.

hypothesis that input charge correlates with both enzyme activity and the generation of two different biochemical products. Importantly, the assembly methods are biologically benign and device operation is enabled without the need for multiple liquid samples. This was envisioned for *in vitro* metabolic or pathway engineering<sup>4,5</sup>. We anticipate that our system and methods can easily be applied in microfluidic devices with embedded microscale electrodes. Indeed, our group has already demonstrated functional enzyme assembly on a chitosan layer, as well as electrochemical small-molecule measurement inside microfluidic channels<sup>4,24</sup>.

A generalized application of the present method is described in the Supplementary Information. We characterized the chip-actuated assembly and attenuation of two additional enzymes: (1) the common reporter  $\beta$ -galactosidase and (2) a microbial transglutaminase used in tissue engineering and other applications<sup>25</sup>. We found that AS(O) acted similarly in oxidizing these proteins and attenuating their activities. We also used *in situ*

electric oxidation of the alternative diffusible redox mediator  $\text{IrCl}_6^{3-}$  to show attenuation of HLPT,  $\beta$ -galactosidase and microbial transglutaminase, with results similar to those obtained with AS. These results, provided in Supplementary Section 11, demonstrate the wider applicability of the method, with the possibility for further expansion.

This study shows that direct electrical control of a diffusible redox mediator at the surface of a gold electrode in the vicinity of an immobilized enzymatic pathway results in predictable protein oxidation, attenuation of activity and biochemical signal generation. We envision that the suite of methodologies demonstrated here can form the basis for targeting and controlling biochemical fluxes of other biohybrid devices. We therefore propose this methodology as a powerful addition to the biofabrication toolbox<sup>26</sup> that furthers the utilization of biologically inspired nanoscale processes by bridging the communications and fabrication gaps that exist between microelectronics and biological systems.

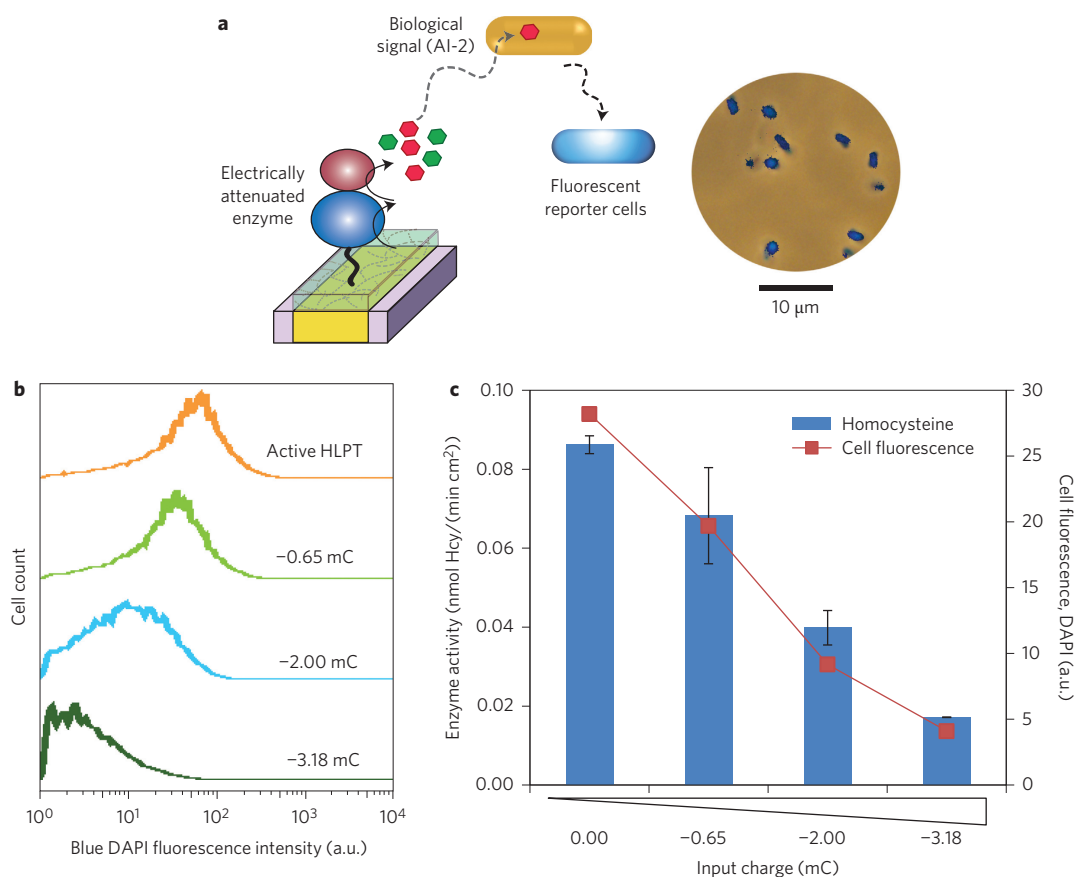


**Figure 4 | *In situ* enzyme attenuation mediates biological signalling.** **a**, Schematic of experiment: HLPT is attenuated *in situ* as in Fig. 3. The generated solution with AI-2 is added to reporter cells, which fluoresce blue. A bright-field image of the cells is overlaid with the blue fluorescent image, showing co-localization of cells and fluorescence. **b**, Histograms from FACS (measuring blue DAPI fluorescence) run on AI-2 reporter cells to which the products of differentially attenuated HLPT-immobilized electrodes were added. **c**, Comparison of the Hcy measured electrochemically and the average blue fluorescence of AI-2 reporter cells from HLPT immobilized on an electrode and attenuated with the indicated input charges. Cell fluorescence averages correspond to those in the histograms in **b**. Three measurements were taken for the activity in **c**, and error bars indicate s.d. The Pearson correlation coefficient for linearity calculated for cell fluorescence versus enzyme activity averages in **c** yielded an  $R^2$  value of 0.98. AI-2, autoinducer-2; Hcy, homocysteine; HLPT, electrically attenuated fusion enzyme; mC, millicoulombs.

## Methods

**Biohybrid device assembly: chitosan film electrodeposition and HLPT conjugation.** A thin layer of chitosan was deposited on a gold-coated silicon chip (electrode fabricated as described in Supplementary Section 1) (cathode) by immersing it with a platinum counter-electrode (anode) into a 0.8% chitosan solution (as described in ref. 27) and applying a current for 2.5 min at  $4 \text{ A m}^{-2}$ . After rinsing the chitosan film with distilled water, tyrosinase at  $300 \text{ U } \mu\text{l}^{-1}$  was mixed with tyrosine-tagged HLPT ( $10 \text{ } \mu\text{M}$  in PBS) and incubated at room temperature for 1 h with the chitosan-coated electrodes. Afterwards, each electrode was briefly rinsed with PBS and kept in the PBS until use. After appropriate treatments (see below), two similarly treated electrodes, facing away from each other, were diagonally immersed in a  $300 \text{ } \mu\text{l}$  solution of  $1 \text{ mM}$  SAH in  $0.1 \text{ M}$  pH 7 phosphate buffer in a standard semi-micro cuvette (Cole Parmer). The cuvette was stoppered and incubated at  $37 \text{ }^\circ\text{C}$  while being shaken at  $100 \text{ r.p.m.}$  for the indicated amount of time to let the enzymatic reaction take place (3–3.5 h). See Supplementary Section 2 for details and diagram of procedure, set-up and chip.

**On-chip biohybrid device electrical attenuation.** For *in situ* attenuation with acetosyringone, the gold chip with HLPT (assembled as above) was used as the working electrode in a three-electrode system with a  $0.5\text{-mm}$ -diameter,  $4\text{-cm}$ -long platinum counter-electrode (Alfa Aesar) and Ag/AgCl reference electrode (BASi). These were placed in a  $250 \text{ } \mu\text{M}$  AS solution and the working electrode biased at  $+0.55 \text{ V}$  using a CH Instruments workstation (CHI 6273c) for the designated amount of time (10–1,000 s). The chip was then rinsed gently with PBS, and allowed to react with SAH as indicated above. See Supplementary Section 2 for a diagram of the set-up.

**Electrochemical homocysteine detection.** To measure the homocysteine generated from an on-chip HLPT, the reaction solution was removed at the end of the incubation with SAH, allowing Hcy measurement. Cyclic voltammetry was used to

detect homocysteine. A three-electrode set-up was used, with a  $2\text{-mm}$ -diameter gold working electrode (CH Instruments) and counter- and reference electrodes as in the attenuation method already described. The potential was swept from  $0 \text{ V}$  to  $+0.7 \text{ V}$  and back at  $50 \text{ mV s}^{-1}$  ( $\sim 28 \text{ s}$ ). The electrodes were cleaned briefly with Piranha solution ( $70\% \text{ H}_2\text{SO}_4$  and  $30\% \text{ H}_2\text{O}_2$ ) before the start of the experiment. Between every measurement the working electrode was polished for 1 min with  $0.05 \text{ } \mu\text{m}$  alumina powder on a felt polishing pad (CH Instruments) and rinsed with distilled water, except during real-time measurement experiments. Integration of the output current yielded the output charge in coulombs ( $Q = \int i \text{ dt}$ ). In the experiments, the total accumulated charge at  $+0.7 \text{ V}$  was recorded and used as a measure of homocysteine.

Received 10 December 2013; accepted 25 June 2014;  
published online 27 July 2014

## References

- Nivala, J., Marks, D. B. & Akeson, M. Unfoldase-mediated protein translocation through an  $\alpha$ -haemolysin nanopore. *Nature Biotechnol.* **31**, 247–250 (2013).
- Moreau, C. J., Dupuis, J. P., Revilloud, J., Arumugam, K. & Vivaudou, M. Coupling ion channels to receptors for biomolecule sensing. *Nature Nanotech.* **3**, 620–625 (2008).
- Mora-Pale, M., Sanchez-Rodriguez, S. P., Linhardt, R. J., Dordick, J. S. & Koffas, M. A. Metabolic engineering and *in vitro* biosynthesis of phytochemicals and non-natural analogues. *Plant Sci.* **210**, 10–24 (2013).
- Luo, X. *et al.* Programmable assembly of a metabolic pathway enzyme in a pre-packaged reusable bioMEMS device. *Lab Chip* **8**, 420–430 (2008).
- Jung, G. Y. & Stephanopoulos, G. A functional protein chip for pathway optimization and *in vitro* metabolic engineering. *Science* **304**, 428–431 (2004).

6. Lee, M. Y., Park, C. B., Dordick, J. S. & Clark, D. S. Metabolizing enzyme toxicology assay chip (MetaChip) for high-throughput microscale toxicity analyses. *Proc. Natl Acad. Sci. USA* **102**, 983–987 (2005).
7. Fernandes, R., Roy, V., Wu, H. C. & Bentley, W. E. Engineered biological nanofactories trigger quorum sensing response in targeted bacteria. *Nature Nanotech.* **5**, 213–217 (2010).
8. Esch, M. B., King, T. L. & Shuler, M. L. The role of body-on-a-chip devices in drug and toxicity studies. *Annu. Rev. Biomed. Eng.* **13**, 55–72 (2011).
9. Service, R. F. Bioengineering. Lung-on-a-chip breathes new life into drug discovery. *Science* **338**, 731 (2012).
10. Huh, D. *et al.* Reconstituting organ-level lung functions on a chip. *Science* **328**, 1662–1668 (2010).
11. Kim, E. *et al.* Redox-capacitor to connect electrochemistry to redox-biology. *Analyst* **139**, 32–43 (2014).
12. Wu, L. Q. & Payne, G. F. Biofabrication: using biological materials and biocatalysts to construct nanostructured assemblies. *Trends Biotechnol.* **22**, 593–599 (2004).
13. Yi, H. *et al.* Biofabrication with chitosan. *Biomacromolecules* **6**, 2881–2894 (2005).
14. Schauder, S., Shokat, K., Surette, M. G. & Bassler, B. L. The LuxS family of bacterial autoinducers: biosynthesis of a novel quorum-sensing signal molecule. *Mol. Microbiol.* **41**, 463–476 (2001).
15. Hardie, K. R. & Heurlier, K. Establishing bacterial communities by ‘word of mouth’: LuxS and autoinducer 2 in biofilm development. *Nature Rev. Microbiol.* **6**, 635–643 (2008).
16. Li, J. *et al.* Quorum sensing in *Escherichia coli* is signaled by AI-2/LsrR: effects on small RNA and biofilm architecture. *J. Bacteriol.* **189**, 6011–6020 (2007).
17. Wu, H. C. *et al.* Biofabrication of antibodies and antigens via IgG-binding domain engineered with activatable pentatyrosine pro-tag. *Biotechnol. Bioeng.* **103**, 231–240 (2009).
18. Lewandowski, A. T. *et al.* Protein assembly onto patterned microfabricated devices through enzymatic activation of fusion pro-tag. *Biotechnol. Bioeng.* **99**, 499–507 (2008).
19. Clement, J.-L., Gilbert, B. C., Rockenbauer, A. & Tordo, P. Radical damage to proteins studied by EPR spin-trapping techniques. *J. Chem Soc. Perkin Trans. 2*, 1463–1470 (2001).
20. Baker, C. J. *et al.* Induction of redox sensitive extracellular phenolics during plant–bacterial interactions. *Physiol. Mol. Plant Pathol.* **66**, 90–98 (2005).
21. Martorana, A. *et al.* A spectroscopic characterization of a phenolic natural mediator in the laccase biocatalytic reaction. *J. Mol. Catal. B* **97**, 203–208 (2013).
22. Hilgers, M. T. & Ludwig, M. L. Crystal structure of the quorum-sensing protein LuxS reveals a catalytic metal site. *Proc. Natl Acad. Sci. USA* **98**, 11169–11174 (2001).
23. Lee, J. E., Cornell, K. A., Riscoe, M. K. & Howell, P. L. Structure of *E. coli* 5'-methylthioadenosine/S-adenosylhomocysteine nucleosidase reveals similarity to the purine nucleoside phosphorylases. *Structure* **9**, 941–953 (2001).
24. Dykstra, P. H., Roy, V., Byrd, C., Bentley, W. E. & Ghodssi, R. Microfluidic electrochemical sensor array for characterizing protein interactions with various functionalized surfaces. *Anal. Chem.* **83**, 5920–5927 (2011).
25. Yung, C. W. *et al.* Transglutaminase crosslinked gelatin as a tissue engineering scaffold. *J. Biomed. Mater. Res. A* **83**, 1039–1046 (2007).
26. Liu, Y. *et al.* Biofabrication to build the biology–device interface. *Biofabrication* **2**, 022002 (2010).
27. Cheng, Y. *et al.* *In situ* quantitative visualization and characterization of chitosan electrodeposition with paired sidewall electrodes. *Soft Matter* **6**, 3177–3183 (2010).

### Acknowledgements

The authors thank the UMD Fischell Department of Bioengineering Core FACS Facility for assistance with FACS data collection and the UMD Nanocenter for providing workspace and tools for electrode fabrication and ICP-EOS measurements. The authors thank Y. Zhou of the UMD Department of Nutrition and Food Science for help with EPR measurements. Financial support for this work was provided by the Defense Threat Reduction Agency (HDTRA1-13-0037), the National Science Foundation (no. 1160005 to WEB, no. 1264509 to HO Sintim) and the RWD Foundation.

### Author contributions

T.G., E.K., G.F.P. and W.E.B. developed the concepts and planned and designed the experiments. T.G., E.K., H.B. and Y.C. fabricated components and performed the experiments and data analysis. J.J.Y., G.F.P., W.E.B. and G.R. supervised the work. T.G., E.K., G.F.P. and W.E.B. wrote and edited the manuscript.

### Additional information

Supplementary information is available in the [online version](#) of the paper. Reprints and permissions information is available online at [www.nature.com/reprints](http://www.nature.com/reprints). Correspondence and requests for materials should be addressed to W.E.B.

### Competing financial interests

The authors declare no competing financial interests.